SLAC–PUB–8312
PPRC-TN-00-02
February 2000

POLARIZED ELECTRON BEAMS WITH P $\geq$ 90%, WILL IT BE POSSIBLE? *

A. V. SUBASHIEV,† J. E. CLENDENIN
Stanford Linear Accelerator Center, Stanford, CA 94309

Abstract

Recent results of electron spin depolarization studies in electron emission from the photocathode semiconductor structures are reviewed. The main mechanisms of electronic depolarization being well understood, a considerable improvement of polarization is expected to be achieved in new superlattice structures, which can be designed to have less depolarization at excitation and in extraction to the surface. Additional polarization growth is expected to be obtained by lowering the operating temperature of the source.

Presented at the
3rd International Workshop on
Electron-Electron Interactions at TeV Energies (e-e- 99),
Santa Cruz, CA, USA
December 10-12, 1999

* Work supported by Department of Energy contract DE–AC03–76SF00515.
† On sabbatical leave from St.-Petersburg State Technical University, Russia

1 Introduction

Accelerated beams of polarized electrons have proven to be extremely useful in a number of high-energy experiments [1]. The techniques used to study the spin structure of the nucleon include elastic electron-nucleon scattering and inelastic reactions induced by polarized electrons. Measurement of the nucleon spin structure functions, obtained from deep inelastic scattering of polarized electrons from polarized nucleon targets were actually the first accelerator-based experiments utilizing polarized electrons [2]. Over the past few years these measurements have been extended to higher values of Q^2 and lower values of the fractional momentum of the parton, $x = Q^2/2M\,\nu$, where Q^2 is the square of the 4-momentum, M is the nucleon mass and ν is the electron energy transfer.

Polarized electron beams have also played an important role in the search for parity non-conservation (PNC). PNC arises from the interference of the electroweak and electromagnetic amplitudes. Left-right asymmetry measurements using polarized electron beams for which the helicity is randomly and frequently reversed are relatively free of systematic errors, and the results are subject to a straight-forward interpretation. The first such measurements using a polarized electron source with a GaAs photocathode provided an unambiguous measurement of PNC consistent with the predictions of the Standard Model (SM) [3]. Similar PNC measurements over a wide range of energies continue to be conducted at several accelerator laboratories with increasingly precise results.

Polarized electrons are expected to play an even more important role in future lepton colliders. At collision energies of $\approx$500 GeV in the center of mass, the cross sections for many processes depend on polarization. A particularly striking example is that the production of W^+W^- pairs, which provide a major part of the background for many other processes, is nearly suppressed for a right-handed electron beam. Within supersymmetry (SUSY), the production of right-handed sleptons and neutralinos dominates for a right-handed beam, whereas left-handed sleptons and charginos dominate for left-handed. Thus polarization will be very useful for sorting out SUSY signals. In addition, precision measurements of properties of SUSY particles will benefit from the background reduction available with right-handed electron beams. Finally, polarized beams enhance the effective luminosity of a collider [4].

Though an electron beam polarization of $\approx$80 %, which is available today, is considered to be sufficient for most high-energy physics experiments, having beams with significantly higher polarization would have an enormous impact on the physics capabilities of a future lepton collider suppressing the background processes and adding a gain in the precision of

measurements[5].

The history of the development of polarized electron sources (PES) consists of close to 25 years of investigations and applications in various fields of modern physics in addition to use in the high-energy physics at a number of accelerator laboratories. Sources of the first generation of solid state PES in early 1980s employed GaAs crystals and films that were able to give polarization of no more than 45 %. A new era of polarized beam experiments began in 1992 when strained semiconductor layers were shown to be effective to obtain polarization values in the range of 75 % - 85 % [6, 7]. The highly polarized electron beam in the Stanford linear collider (SLC) provided a measurement of the weak mixing angle, $\sin^2\theta_W^{\rm eff}$, with a precision of $\approx$0.1 % [8]. Since then PES based on photoemission from GaAs strained thin films are proven to be highly reliable systems meeting all accelerator requirements for charge, stability, and reliability [9].

Attempts to reach further improvements in polarization by optimization of the same type of semiconductor structures did not give noticeable results. Nonetheless recent investigations of physical processes in semiconductor cathodes and studies of new cathode structures have proven helpful in clarifying the limits of present cathodes and in choosing the way to further progress. The general status of semiconductor PES development, and the main spin depolarization mechanisms were discussed in recent reviews [4, 10]. The purpose of this survey is to draw together the results of the latest investigations of the basic processes controlling the polarization losses in photocathodes in order to reestimate the perspectives for a further increase of the electron beam polarization. Polarized electron photoemission from a thin semiconductor layer is understood as a muli-step process (illustrated in Fig. 1), which consist of (i) optical interband absorption with electron excitation to the conduction band, (ii) transport to the surface and capture in the surface band bending region (BBR), (iii) electron dynamics in the BBR, which is predominantly energy relaxation, and (iv) electron emission in vacuum.

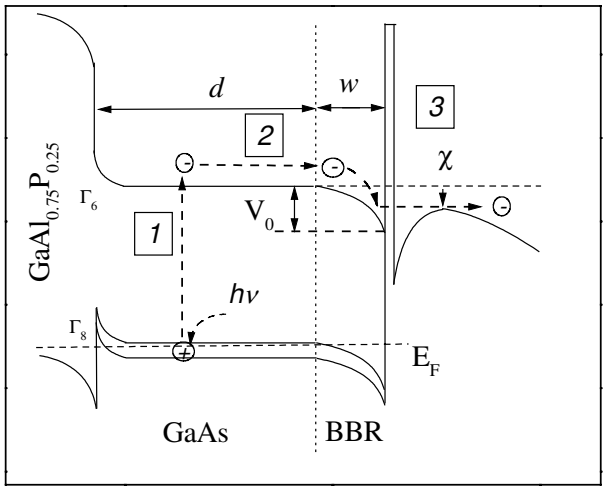

Figure 1: Energy band diagram of a strained GaAs active layer illustrating multi-step electron emission.

The electron polarization is manifest by the unequal population of the

two electron spin states $|\uparrow>$ and $|\downarrow>$ and is defined by $P = (n_\uparrow - n_\downarrow)/(n_\uparrow + n_\downarrow)$, where $n_\uparrow$ ($n_\downarrow$) is the number of electrons with the spin parallel (antiparallel) to the propagation direction of the incident light. According to the multi-step emission model, the processes at different stages of the photoemission have strongly different time scales, and are essentially independent, so that the polarization P of the emitted electrons can be expressed as a product of the factors reflecting each step of the emission process,

$$P(h\nu) = P_0(h\nu) R_{\rm tr} R_{\rm BBR} R_{\rm emi}, \tag{1}$$

where $P_0(h\nu)$ is the electron polarization in the conduction band at the excitation moment, the factors $R_{\rm tr}$, $R_{\rm BBR}$, and $R_{\rm emi}$ describe spin relaxation during each of the subsequent stages of emission as listed above. These stages can be investigated separately using the most suitable structures and techniques.

2 Electron Polarization at the Moment of Optical Excitation

The polarization of electrons in semiconductors at the moment of optical excitation is based on optical spin orientation of electrons when the crystal is pumped by circularly polarized light. The main features of optical spin orientation come from the spin-orbital splitting of the degenerate states of the valence band maximum. These states belong to a $J = \frac{3}{2}$ 4-fold multiplet. With circularly polarized light, two simultaneous transitions changing the electron angular momentum by unity are excited resulting in the unequal population of two conduction band states $S_z = \frac{1}{2}$ and $S_z = -\frac{1}{2}$. In the early 1990s two efficient ways to populate only one conduction band spin state were experimentally demonstrated, both based on the splitting of the $J = \frac{3}{2}$ multiplet states.

One way is to employ semiconductor structures with strained thin films where the lattice mismatch generates substantial stress in the overlayer. The stress lifts the orbital degeneracy of the $P_{3/2}$ multiplet at the valence band edge into light- and heavy-hole subbands. A lattice mismatch of typically 1% results in a splitting of the heavy and light valence band states by about 0.05 eV.

The second way is based on hole confinement in the structures forming quantum wells (QW) for the holes, since the ground state energy for the heavy and light holes in a well is different. The energy splitting of the heavy and the light hole ground states strongly depends on the depth of the QW and is typically of the same magnitude as in strained thin films. These two ways to split the valence band are combined in strained-layer superlattices

[11, 12, 13]. For either technique the heavy hole band can be chosen (and usually is) to be at a higher energy than the light hole, which gives potentially a much larger splitting.

Typical experimentally observed [14] spectral curves of the polarization and the quantum yield from a strained layer photocathode at the absorption edge are shown in Fig. 2. The characteristic features of the $P(h\nu)$ and $Y(h\nu)$ curves are polarization enhancement in the region of one-band absorption, fast decay of polarization both at the high energy side, when $h\nu > E_g + \Delta$, and at $h\nu < E_g$. At the high -energy side of the maximum, the light-hole band starts to contribute to electron generation. Therefore the polarization approaches the limiting value 50 % as it would for unstrained material with an unsplitted valence band.

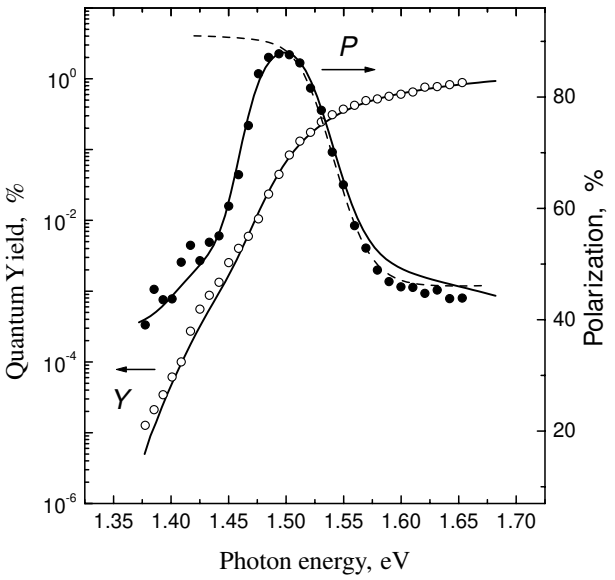

Figure 2: Electron spin polarization and quantum yield spectra for a strained layer cathode. Experimetal data (points) compared with resuts of the calculations(solid lines), dotted line is calculations without allowance for the tails and phonon-assisted transitions, from Ref. 14.

More informative is the polarization decrease in the region of the absorption edge. Possible mechanisms include the generation of electrons in band tail states of conduction band with longer lifetime and therefore stronger spin relaxation, generation of electrons from the band tail states of the light-hole band and last but not least, phonon-assisted absorption with the changing of the hole momentum state. To discriminate between these possibilities the emission curves, $P(h\nu)$ and $Y(h\nu)$ were calculated in ref. [14] for a number of samples together with the curves for polarized luminescence. These calculations and comparison with the experiment (shown in Fig. 2) indicated that the reduction of polarization is mostly due to the phonon-assisted processes, since only this mechanism is able to reproduce the spectral curve dependence in the region ≈ 40 meV below the absorption edge, characteristic for these transitions. The value of the initial electron polarization in the polarization maximum (for the sample in Fig. 2) is ≈ 94 %.

These polarization losses are enhanced in highly p-doped samples where band tailing and mixing of the hole states is induced by the random potential distribution of the ionized acceptor centers.

Note that the second-order excitation processes are suppressed at low temperatures

(since only the processes with optical phonon absorption are important near the absorption edge) and in the structures with higher valence band splitting for which the distance to the intermediate light-hole state is enlarged. This feature can be used to reduce this source of polarization losses.

3 Electron Transport to the Surface

This stage of the emission process can be fairly well studied by an investigation of the emission from the samples with different active layer thicknesses and also by time-resolved measurements, when the electrons with different time of escape to the surface region are registered. These experiments show that the main transport mechanism is diffusion to the surface, which is limited by the finite surface recombination time. Therefore in thin films with $d << L$ (where d is the layer thickness and L is the diffusion length) the escape time from the active layer equals $\tau_{\rm esc} = d/S$, S being the surface recombination velocity [15] The corresponding depolarization factor is in general described by

$$R_{tr} = \frac{\tau_s}{\tau_{\rm esc} + \tau_s}, \tag{2}$$

where τ_s is the spin relaxation time in the active layer.

The experimental data for the maximum polarization values from Refs. [16, 17] together with the dependence of eq. (2) (multiplied by a factor of 0.93 to account for the polarization losses in other steps of the emission) for typical S and τ_s values ($S = 2 \times 10^6$ cm/s, $\tau = 50$ ps), are shown in Fig. 3. Given the experimental data in Fig. 3 the polarization losses in this step are typically $\approx$ 7 % for 100 nm layers. Since τ_s is known to decrease at low temperatures in low-doped samples, the polarization losses can be also reduced.

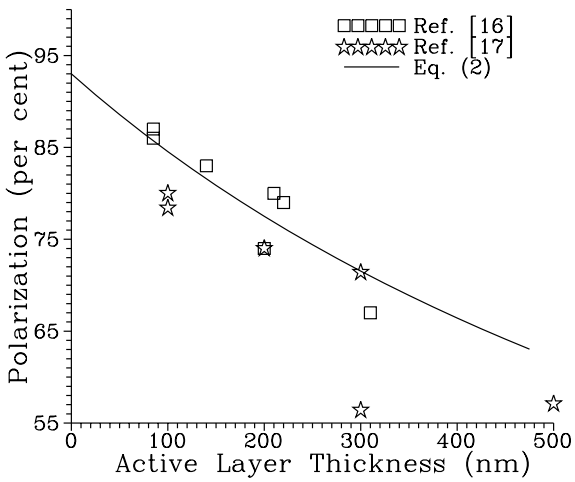

Figure 3: Emitted electron polarization as a function of strained layer thickness.

4 Electron Kinetics in BBR Region

The polarized electron emission can be obtained if the surface barrier for the electrons is strongly lowered by Cs (O) activation to allow the electrons to escape into vacuum. The electron energy distribution curves (EDC) measured by several groups and using different activation procedures (e.g. see Refs [18, 19, 20]) indicate that a predominant portion of the photoelectrons are emitted in vacuum with energy below the bottom of the conduction band, that is, from the energy levels in the band bending region (BBR) at the surface. The distribution is not altered considerably in a fairly broad interval of excitation energy variation, which indicates that electrons are rapidly captured in the BBR and have time for energy relaxation before emission into vacuum. The electron kinetics in the BBR are still a field for experimental investigation and theoretical study, since the structure of the activation layer and the details of the electron density of states in the BBR are not well established.

Monte-Carlo modeling of the spatial distribution of the electron potential in the BBR [22] showed large fluctuations of the potential, which results from random spatial distribution of ionized acceptors and Cs-originated ionized donor centers. As a result most of the states in the BBR below a certain level called a mobility edge (ME) are localized also in the surface plane by the potential fluctuations. The density of surface localized states $g(\epsilon)$ below the ME should be a rapidly decreasing function of the localization energy ϵ in the band gap.

The experimental results can be analyzed in terms of a model that considers the EDC formation as a result of competition between the two following processes: phonon assisted electron hopping between the localized tail states and electron emission in vacuum.

Since the experimentally observed width of the EDC curves exceeds the characteristic energies of the phonons in GaAs, the energy relaxation can be considered as a drift down in energy. It is then possible to describe the energy relaxation for the electronic surface density $n(\epsilon)$ by a Fokker-Planck type equation:

$$\frac{dn}{dt} = -\delta \frac{\partial}{\partial \epsilon} \left(\frac{n(\epsilon)}{\tau(\epsilon)} \right) - \frac{n(\epsilon)}{\tau_{emi}}. \tag{3}$$

In this equation the first term describes the flow of electrons through the states with energy ϵ: $n(\epsilon - \delta)/\tau(\epsilon - \delta) - n(\epsilon)/\tau(\epsilon)$, and the second one is just the emission current $J_{emi}(\epsilon)$. In stationary conditions $dn/dt = 0$, and one obtains the energy dependence of the emission current in the BBR, which we write down for the case of exponential conduction band tailing in the BBR,

$$J_{emi}(\epsilon) = J_{emi}(0) \exp[\frac{\epsilon}{\gamma} - \alpha(\exp(\frac{\epsilon}{\gamma}) - 1)]. \tag{4}$$

Here γ is the width of the tail state region, the parameter α is given by $\alpha = (\gamma/\delta) \times (\tau(0)/\tau_{emi})$, δ is the emitted phonon energy, $\tau(0)$ is the emission time of the optical phonon at the edge of the conduction band, and $\tau_{\rm emi}$ is the electron emission time in vacuum.

The experimental EDC curves for the strained GaAs layers are shown in Fig. 4, together with electron polarization data. The calculated EDC curves using eq. (4) for reasonable (theoretically motivated) values of the parameters of the model are found to be in excellent agreement with the experimental data. Note that polarization of the emitted electrons does not decrease with decreasing electron energy, which could be expected from the well established experimental result for the case of high-energy excitation in the electron energy region above the conduction band edge in the bulk.

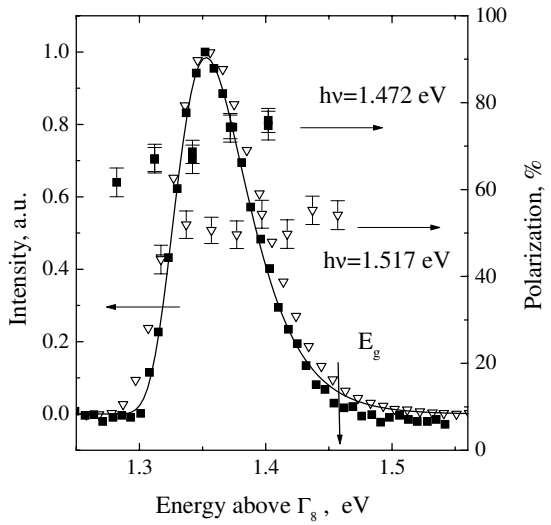

Figure 4: Experimental electron energy distribution curves for GaAs strained layer cathode, T = 300 K, together with the polarized electron distibution data for two values of the excitation energy. Figure from Ref. 21.

This experimental finding is completely in line with the model of localized states at the surface: the main spin-relaxation mechanism of D'yakonow-Perel (DP) (see Refs. [4, 10]) is suppressed for the localized states below ME due to the effective averaging of the odd in k-vector terms in the DP Hamiltonian at all directions, so that $< k_i k_j k_l >= 0$, and the weak overlap of the electron localized states with hole states, which are situated outside from the BBR, makes Pikus-Aronow-Bir relaxation due to electron scattering on the holes ineffective.

Thus, very high doping of the surface layer will not cause depolarization of emitted electrons. This conclusion is important for emission of high intensity electron bunches when surface charge limitation effects are observed [23], since the way to reduce these effects is by high doping of the BBR region layer.

5 Electron Emission in Vacuum

A separate contribution to the electron depolarization can be expected from the electron emission in vacuum. This depolarization can be understood in terms of the spin precession in the effective magnetic field associated with the potential at the surface, i.e. BBR potential

and the potential V of the effective surface barrier. Then depolarization is caused by the random termination of this precession when tunneling in vacuum occurs. To illustrate this mechanism consider the Hamiltonian of the spin-orbital interaction at the surface,

$$H^i = U(z) - \frac{\hbar}{4m^2c^2}\left(\sigma[\mathbf{p}\times\mathbf{n}]\right)\frac{dV}{dz}. \tag{5}$$

It is convenient to choose the quantization axis to be directed perpendicularly to the plane of the local electron movement (which is formed by the normal to the surface plane $\mathbf{n}$ and the electron local momentum $\mathbf{p}$) since then the Hamiltonian (5) is diagonal and does not lead to the spin flip processes. In this approach the electron depolarization $R_{\rm emi}$ is due to the difference in the transmission amplitudes, δ, for two spin states, $R_{\rm emi} \approx 1 - 2\delta^2$. The effective magnetic field at the surface is enhanced in the narrow-band semiconductors with splitted valence band. In this case the effective Hamiltonian can be written in the form [24]

$$H(z) = \left(\sigma[\mathbf{p}\times\mathbf{n}]\right)\delta(z-z_0)F(z). \tag{6}$$

Here

$$F(z) = \frac{\Delta_{so}(z)\hbar P^2}{3(E-\epsilon_v(z))(E-\epsilon_v(z)+\Delta_{so}(z))}, \tag{7}$$

where E is the electron energy, $\Delta_{so}(z)$ is spin-orbital splitting of the valence band, and $\epsilon_v(z)$ is the valence band energy. Straightforward calculations of the transmission amplitudes and then the electron polarization showed that for parameters of the BBR in GaAs these losses can not exceed 1 % and can be neglected.

6 Superlattice-based Photocathodes

For the single-layer cathodes the accessible range of variation of their parameters appeares to be very narrow. Therefore the most promising way to further improvements in polarization is to use new superlattice (SL) structures, especially the so-called strained short-period SLs [11, 12, 13]. They consist of several (10-20) thin strained films (for example, InGaAs or AlInGaAs) separated by layers of unstrained larger-bandgap material (GaAs or AlGaAs), specially designed to build quantum wells the holes but keep electron mobility high. The benefits of SL structures are the additional valence band splitting caused by the hole localization in SL quantum wells and the possibility of a very high surface layer doping while active layer is made low doped (so-called modulation doping). Thus, very high polarization values obtained with strained SL structures were already reported in Ref. [11]. In a new $Al_xIn_y\ Ga_{1-x-y}As/GaAs$ SL structure for the photocathodes proposed in Ref. [13] polarization as high as 86 % was reproducibly obtained in addition to high quantum efficiency

(QE) at the polarization maximum. In both cases precise modulation doping was exploited, providing reduced polarization losses at the excitation and extraction to the surface. The SL structures have high flexibility allowing polarization losses at subsequent stages of the emission to be minimized. Besides, variation of the SL structure parameters makes possible to optimize the cathode structure as a whole, following band structure engineering concepts. Active research in this direction is on the way.

7 Conclusions

Analysis of the emission processes in PES show that the polarization losses associated with the electron stay in the crystal can be reduced if one uses only electrons with a lifetime much shorter that the spin relaxation time for a given step of emission. This can be realized in a number of ways, starting with defects-enriched crystals with anomalously short electron lifetimes to the emission from the sructures with lowered QE when only fast electrons which do not have much time for spin relaxation are emitted. These improvements come with a price of a strong decrease in the number of emitted electrons. The other way is to use less doped samples and low temperatures to slow spin relaxation.

Two processes can not be avoided in principle: electron optical excitation and electron emission into vacuum. Fortunately, there is no experimental indication of the polarization losses during this latter process and no theoretical reasons for such losses to be large unless the surface is polluted with magnetic defects. Therefore the polarization at excitation sets an ultimate limit for the electron polarization.

Thus, from the discussion above, the prescription to make the emitted electron polarization above 90 %, while not simple, yet appears possible: design new structures to have a high valence band splitting (exceeding the optical phonon energy), use a low doping in the active region and lower the operational temperature to suppress light-hole heavy-hole state mixing and spin relaxation. These possibilities will be investigated in the nearest future.

Acknowledgments

AS thankfully acknowledges the hospitality extended to him during his stay in SLAC.

References

[1] See e.g. *Proc. of 12th Intern. Symp. on High-Energy Spin Physics* (SPIN 96), Amsterdam, 1996, eds. C. W. de Jager et al. (World Scientific, 1997).

[2] M. J. Alguard et al., *Phys. Rev. Lett.* **37** (1976) 1261.

[3] C. Y. Prescott et al., *Phys. Lett.* B **77** (1978) 347.

[4] J. E. Clendenin, *Int. J. Mod. Phys.* A **13** (1998) 2507.

[5] M. Woods (1999), these proceedings.

[6] T. Maruyama, E. L. Garwin, R. Prepost et al., *Phys. Rew. Lett.* **66** (1991) 2376.

[7] T. Nakanishi, H. Aoyagi, H. Horinaka et al. *Phys. Lett.* A **158**(1991) 345.

[8] For the latest data see e.g. M. Woods, SLAC-PUB-8143, May 1999.

[9] R. Alley et al., *Nucl. Instr. and Meth.* A **365** (1995) 1.

[10] A. V. Subashiev, Yu. A. Mamaev, Yu. P. Yashin, J. E. Clendenin, *Phys. Low-Dim. Struct.* **1/2** (1999) 1, [also SLAC-PUB-8035, Dec. 1998].

[11] T. Nakanishi, in *Polarized Gas Targets and Polarized Beams, 7th Intern. Workshop*, Urbana, 1998, eds. R. Holt et al., AIP Conf. Proc. **421** (1997) 300.

[12] Yu. A. Mamaev et. al., *Phys. Low-Dim. Struct.* **10/11** (1995) 61.

[13] A. V. Subashiev et al., in *Proc. of 24ht Int. Conf. on Physics of Semiconductors* (ICPS-24), Jerusalem, 1998 [also SLAC-PUB-7922, Aug. 1998].

[14] A. V. Subashiev et al., *Semiconductors* **33** (1999) 1182.

[15] B. D. Oskotskij et al., *Phys. Low-Dim. Struct.* **1/2** (1997) 77.

[16] H. Aoyagi et al., *Phys. Lett.* A **167** (1992) 415.

[17] R. Mair et al., *Phys. Lett.* A **212** (1995) 231.

[18] H.-J. Drouhin, C. Hermann, G. Lampel, *Phys. Rev.* B **31** (1985) 3859.

[19] A. S. Terekhov, D. A. Orlov, *SPIE* **2550** (1995) 157.

[20] A. W. Baum et al., *SPIE* **2550** (1995) 189.

[21] Yu. A. Mamaev et al., *Sol.State Comm.* (2000), in press.

[22] B. D. Oskotskij, A. V. Subashiev, L. G. Gerchikov, in *Polarized Gas Targets and Polarized Beams, 7th Intern. Workshop*, Urbana, 1997, eds. R. Holt et al., AIP Conf. Proc. **421** (1998) p. 491.

[23] H. Tang et al. in *Proc. of the 4-th European Particle Accelerator Conf.*, London, 1994, eds. V. Suller et al. (World Scientific, 1994), p. 46.

[24] L. G. Gerchikov, A.V. Subashiev, *Sov. Phys. Semicond.* **26** (1992) 73.